Three-Dimensional Unsteady Laminar Shock-Wave / Boundary Layer Interaction

J.-Ph. Boin [(1)]
J.-Ch. Robinet [(2)]
[(1)] LEA CEAT 43, route de l'Aérodrome 86036 Poitiers Cedex
[(2)] SINUMEF ENSAM/Paris 151, Bd. de l'Hôpital 75013 PARIS

Jean-Christophe.Robinet@paris.ensam.fr

ABSTRACT

The objective of this work is to describe, in a very simple geometrical configuration, some physical mechanisms at stake in an unsteady shock-wave / boundary layer interaction (SWBLI). 3D unsteady Navier-Stokes equations are numerically solved with a dual time step AUSM+ scheme. The conditions to obtain an unsteady SWBLI will be discussed. More precisely we want to show that unsteadiness has originates not only in turbulence but also in the existence of instabilities inside the separated boundary layer.

1.0 INTRODUCTION

The knowledge of the boundary layer which develops on the walls of aeronautical devices like a retreating part of airplane, of missile, or of air intakes of engines, is essential to optimise the use of these vehicles or equipments. The separation of this boundary layer or its disturbance by a shock wave are two phenomena which can involve important losses of effectiveness, and thus to prove particularly harmful. For example, the design of a vehicle at high speeds, extremely expensive, requires the taking into account of the consequences of such disturbances on the performances of the machine. The study of an interaction between an oblique shock wave and a turbulent (or not) supersonic boundary layer should bring many informations on this subject. In particular when the SWBLI is non-stationary.

In the literature, two *scenarii* are opposed for the interpretation of the low frequencies self-sustained oscillations which develop in SWBLI when the interaction becomes high: a first scenario is to seek the origin of the oscillations in the nature of turbulence in the boundary layer, more precisely in the interaction of the upstream coherent structures with the shock. In the second scenario, the oscillations originate in the intrinsic dynamics of the separated zone. Although in the second scenario, turbulence plays necessarily a part. Even if the boundary layer is laminar upstream, the interaction can become transitional if the shock is strong enough. So the structure of the flow can be modified qualitatively. However, in this scenario, the low frequency dynamics of the shock/boundary layer system originates in the existence of intrinsic instabilities in the separated zone quasi independently of the boundary layer turbulent nature. It is within the framework of this second scenario that this article is.

The objective of this work is to demonstrate that the low frequency behaviour experimentally observed in SWBLI can be linked to the intrinsic dynamics of the detached zone induced by the interaction, independently of the boundary layer turbulent characteristics. To this end, it was decided to study the evolution of the interaction between an incident shock wave and a laminar boundary layer developing over a flat plate when the incident shock angle is gradually increased, while keeping constant the free stream Mach number and the Reynolds number. The interaction of an oblique shock wave with a laminar

Paper presented at the RTO AVT Specialists' Meeting on "Enhancement of NATO Military Flight Vehicle Performance by Management of Interacting Boundary Layer Transition and Separation", held in Prague, Czech Republic, 4-7 October 2004, and published in RTO-MP-AVT-111.

Report Documentation Page

Form Approved
OMB No. 0704-0188

1. REPORT DATE	2. REPORT TYPE	3. DATES COVERED
01 OCT 2004	**N/A**	**-**

4. TITLE AND SUBTITLE	5a. CONTRACT NUMBER
Three-Dimensional Unsteady Laminar Shock-Wave / Boundary Layer Interaction	5b. GRANT NUMBER
	5c. PROGRAM ELEMENT NUMBER
6. AUTHOR(S)	5d. PROJECT NUMBER
	5e. TASK NUMBER
	5f. WORK UNIT NUMBER
7. PERFORMING ORGANIZATION NAME(S) AND ADDRESS(ES) **LEA CEAT 43, route de lAérodrome 86036 Poitiers Cedex; SINUMEF ENSAM/Paris 151, Bd. de lHôpital 75013 PARIS**	8. PERFORMING ORGANIZATION REPORT NUMBER
9. SPONSORING/MONITORING AGENCY NAME(S) AND ADDRESS(ES)	10. SPONSOR/MONITOR'S ACRONYM(S)
	11. SPONSOR/MONITOR'S REPORT NUMBER(S)

12. DISTRIBUTION/AVAILABILITY STATEMENT
Approved for public release, distribution unlimited

13. SUPPLEMENTARY NOTES
See also ADM201868, RTO-MP-AVT-111 Enhancement of NATO Military Flight Vehicle Performance by Management of Interacting Boundary Layer Tranisition and Separation (L'amelioration des performances des vehicules aeriens militaires de l'OTAN par la gestion de l'interaction entre la transition et le decollement de la couche limite)., The original document contains color images.

14. ABSTRACT

15. SUBJECT TERMS

16. SECURITY CLASSIFICATION OF:			17. LIMITATION OF ABSTRACT	18. NUMBER OF PAGES	19a. NAME OF RESPONSIBLE PERSON
a. REPORT	b. ABSTRACT	c. THIS PAGE			
unclassified	**unclassified**	**unclassified**	**UU**	**10**	

Standard Form 298 (Rev. 8-98)
Prescribed by ANSI Std Z39-18

boundary layer over an adiabatic flat-plate is computed, see Figure 1. The test-case considered has been experimentally and numerically studied by Degrez *et al.* [2]. The freestream Mach number is 2.15 for the numerical simulation. The Reynolds number based on the distance X_{sh} between the plate leading edge and the shock impingement point is 10^5. The shock angle with respect to the horizontal is initially equal to θ =30.8°, which corresponds to a shock generator angle of 3.75°. This dataset takes into account confinement, 3D effects and measurement approximations; it is not strictly the same as the experiment freestream conditions. The evolution of the SWBLI when the incident shock angle increases is a very complex problem. Indeed, for a particular value of the angle θ, the flow becomes transitional in the interaction zone. This transitional state will probably modify substantially the topology and the temporal dynamics of the interaction zone. In this article, three-dimensional computations will be done without taking into account the transitional character of the flow.

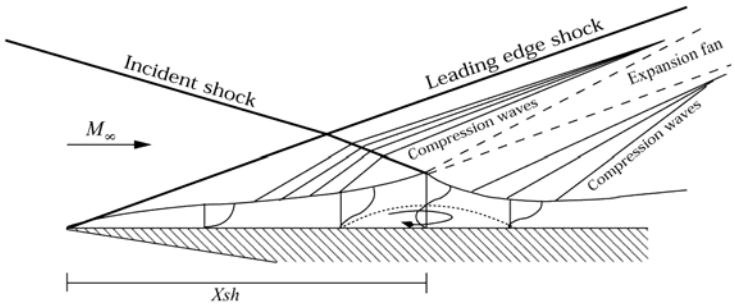

Figure 1: Scheme of the shock/boundary layer interaction

2.0 NUMERICAL METHODS

A numerical solution of the shock-wave/laminar boundary-layer interaction is obtained by solving the 3D unsteady compressible Navier-Stokes equations written in conservative form:

$$w_t + \left(f^E - f^V\right)_x + \left(g^E - g^V\right)_y + \left(h^E - h^V\right)_z = 0 \qquad (1)$$

where $w = (\rho, \rho u, \rho v, \rho w, \rho E)^T$ is the state vector expressed in terms of the conservative variables density, momentum and total energy, $f^E = f^E(w)$, $g^E = g^E(w)$ and $h^E = h^E(w)$ are the Euler fluxes, $f^V = f^V(w, w_x, w_y, w_z)$, $g^V = g^V(w, w_x, w_y, w_z)$ and $h^V = h^V(w, w_x, w_y, w_z)$ stand for the viscous fluxes in the three space directions. The inviscid fluxes are approximated using the AUSM+ scheme developed by Liou and Edwards (1998). The use of a third-order MUSCL reconstruction of the vector of primitive variables $(\rho, u, v, w, p)^T$ ensures high-accuracy.

Second-order accuracy in time approximate solution of system (1) is obtained using an implicit linear multi-step method. An implicit treatment based on a matrix-free point-relaxation method is used; see Boin *et al.* [1] for more details.

The incoming supersonic flow is imposed on the inlet plane x=0. At the exit plane, the conservative variables are extrapolated at the first-order from the values at the nearest upstream location. The flat-plate is assumed to be an adiabatic wall where velocity vector is zero; pressure is extrapolated at first-order from the values just above the plate. Periodic boundary conditions are used on the lateral planes; Figure 2.

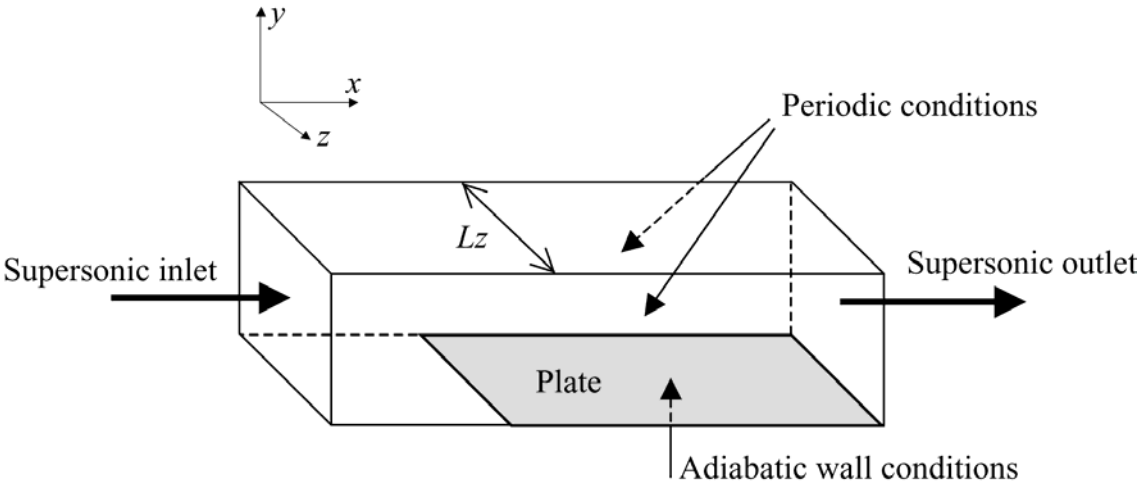

Figure 2: Three-dimensional computational domain and boundary conditions

3.0 THREE-DIMENSIONAL UNSTEADY COMPUTATIONS

The objective is to study the appearance of 3D unsteady flows in the case of a shock/boundary layer interaction and to describe topologic and dynamic characteristics inside and outside the interaction. We choose to change the incident shock angle without changing the shock impingement point. In this condition, the Reynolds number will be the same as Degrez one. The objective is to show that a low frequency self-maintained unsteady state can be reached in a fully laminar flow.

3.1 Introduction

The 2D and 3D SWBLI have been previously computed for different incident shock angle from 30.8° up to 31.7° and these computations have shown that for θ<31.7° the SWBLI remains two-dimensional and stationary for all *Lz* (Boin *et al.* [1]). Figure 3 Synthesize the results previously obtained.

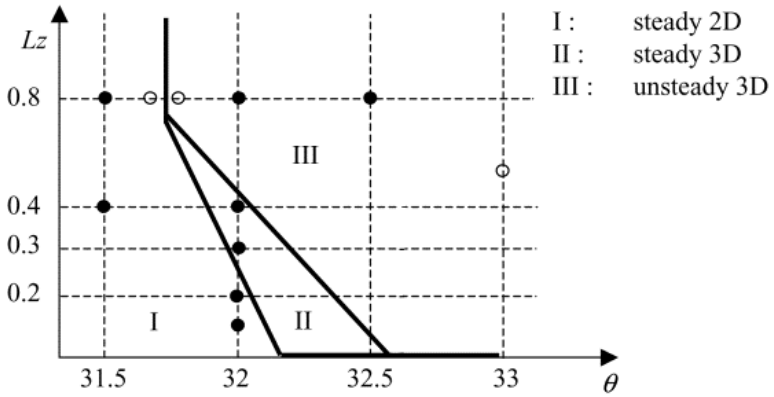

Figure 3: Flow organization according to the incident shock angle and the transverse size of the computational domain.

In this paper, the incident shock angle θ is constant and equal to 32° and only the spanwise *Lz* is modified.

Two computational domains have been used: $D_1=[0;2]\times[0;1.25]\times[0;L_z]$ and $D_2=[0;2.2]\times[0;1.25]\times[0;L_z]$. The grid is composed respectively of $240\times115\times40$ points for D_1 and $270\times115\times40$ points for D_2, which allows having the same mesh size in the *x*-*y* directions. Upstream characteristics remain the same and boundary conditions are the one described in §2. The goal of this section is to characterize the spontaneous appearance of the 3D instabilities according to transversal dimension. Computations have been realized with a spanwise *Lz* varying from *0.1* to *3*, only the most representative cases are presented here.

3.2 3D steady bifurcations

When the transverse dimension is smaller than 0.2 times the interaction length X_{sh}, the flow is still two-dimensional and stationary. When *Lz* =0.2, the first bifurcation observed is a steady three-dimensional one. On Figure 4, the left graph shows a surface streamlines visualization on the plate for *Lz* =0.2 (flow coming from the left). These are quasi-parallels to the freestream. We observe the detachment and reattachment line on the plate; they are perpendicular to the freestream. On Figure 5, the left graph shows a 3D view from the inside of the bulb. The surface streamlines appears on the plan *y*=0 and on a median plan *z*=constant. The streamlines are represented in 3D by ribbons of which the color is a function of the transverse velocity amplitude |*w*|. The *y*-scale is zoomed 10 times with regard to the flow direction; the *z*-scale is dilated 5 times. Even for *Lz =0.2*, the 3D character appears spontaneously, but the transverse velocity amplitude remains weak ($10^{-3}\,V_\infty$). For a larger spanwise length *Lz*, the order of amplitude of *w* is completely comparable to that of *u* or *v* inside the bulb. Results are presented in Figure 4 and Figure 5 (right) for a spanwise *Lz* equal to 0.4. The detachment line is slightly curved whereas the reattachment line undergoes a strong deformation. The 3D character occurs also inside the recirculation zone with the appearance of two counter rotating vortex tubes which take some fluids of the wall to move to the shear layer. More precisely, every tube originates slightly upstream to the interaction line (X_{sh} =1) from the *xz*-plan, and ends up feeding the main recirculation zone in the *xy*-plan. Figure 6 shows an iso-surface of zero longitudinal velocity. It describes the 3D envelope of the recirculation zone. Inside, streamlines go back up the main stream. At *Lz =0.4*, this envelope is strongly deformed with regard to its equivalent in 2D. We notice a kind of plucking near the lateral edges of the domain. In this place the height of the bulb is 5 times weaker than in the middle of the domain.

For greater spanwises, the flow becomes 3D and unsteady. These particular cases are handled in the following section. The study of the transitory phase of unsteady 3D cases θ=32°, $Lz \geq 0.8$, is going to give us more information about the coexistence of the different 3D instabilities.

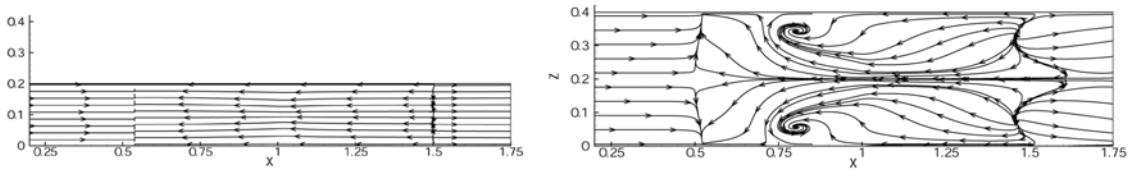

Figure 4: Surface streamlines on the plate, *Lz* =0.2 (left), *Lz* =0.4 (right), θ=32°

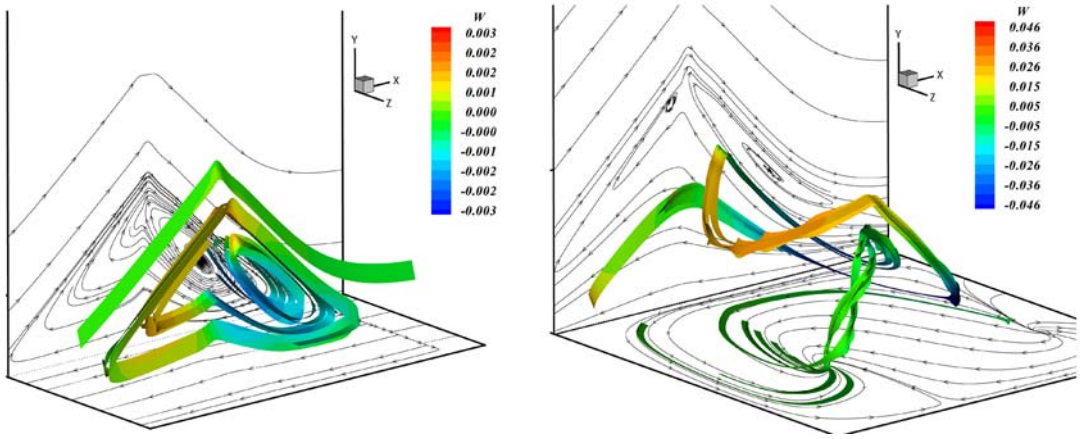

Figure 5: 3D view inside the bulb, *Lz* =0.2 (left), *Lz* =0.4 (right), θ=32°

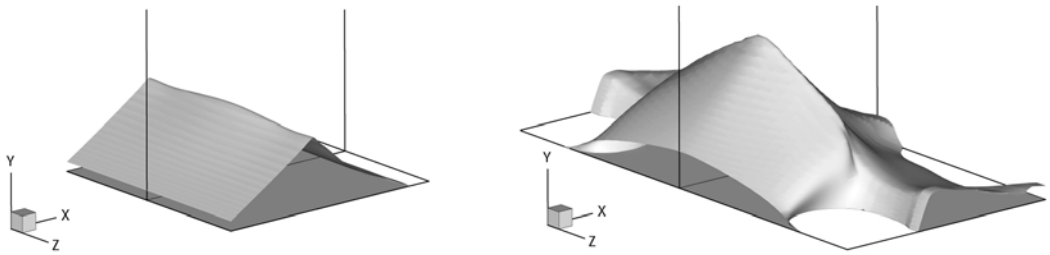

Figure 6: Bulb envelope, *Lz* =0.2 (left), *Lz* =0.4 (right), θ=32°

3.3 3D unsteady behaviour

When the incident shock angle is equal to 32° and the spanwise length up to 0.8, the flow is 3D and unsteady. However the appearance of the unsteadiness is not made in a direct way. Figure 7 and Figure 8 show the time evolution of the unsteady residual for two different spanwise lengths, 0.8 and 1. The progress towards the monotonous unsteady state contains several stages which can be connected with different instabilities. Figure 8 confirms that an established system is reached and is purely periodic.

The case *Lz*=0.8 is discuss here, for *Lz*=1, the topologic aspects are closely similar. Surface streamlines and 3D views are presented in Figure 9 and Figure 10 for different moments (I to V). On 3D views, the y-scale is dilated 16 times while it is dilated 10 times on the envelopes, Figures 11. The z-scale is dilated 5 times always with regard to the stream direction. During the first phase from *t*=0 to *t*=16 ms, the flow remains two-dimensional and stationary (I). Then a first bifurcation appears in the residual evolution. We can see quasi-steady 3D instabilities growing up with transverse wavelengths about 0.4 while the z-dimension *Lz* is 0.8 (II and III). Then four counter rotating vortex tubes similar to those described in the previous paragraph appear (III). At this moment (*t*=35ms) two instabilities are simultaneously present with different wavelengths, 0.4 and 0.8. This coexistence is not the last. From *t*=44ms, the instability with the shortest wavelength disappears (IV). The residual decreases then of 2 orders up until *t*=58ms when a second bifurcation leads the flow toward an unsteady state (V). The unsteady results show a beating movement of the bulb in the *xy*-plan. This phenomenon is combined with a transverse movement accompanied by an asymmetry (V). The size and shape evolution of the bulb is presented Figure 11. 2D at first, the envelope becomes ondulated with a wavelength twice as small as the transverse size. The total volume keeps about the same (II). From t=35ms (III), the instability of wavelength 0.8 is going to take over the other and give the bulb its final shape (IV). By comparing the surface streamlines and the envelopes, the bulb has increased in the *x* and *y* directions but not in a uniform way. The volume remains globally the same. The envelope shape is a succession of nodes and antinodes.

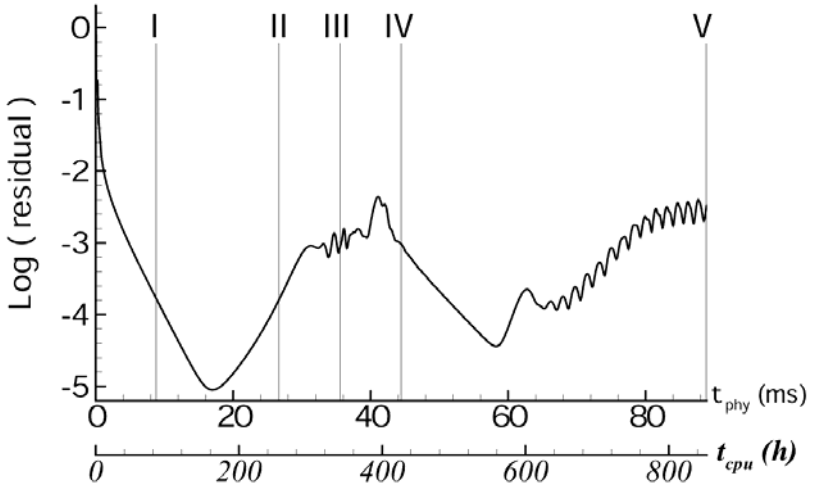

Figure 7: Residual time evolution and CPU time on a 2.4GHz Pentium processor, *Lz*=0.8

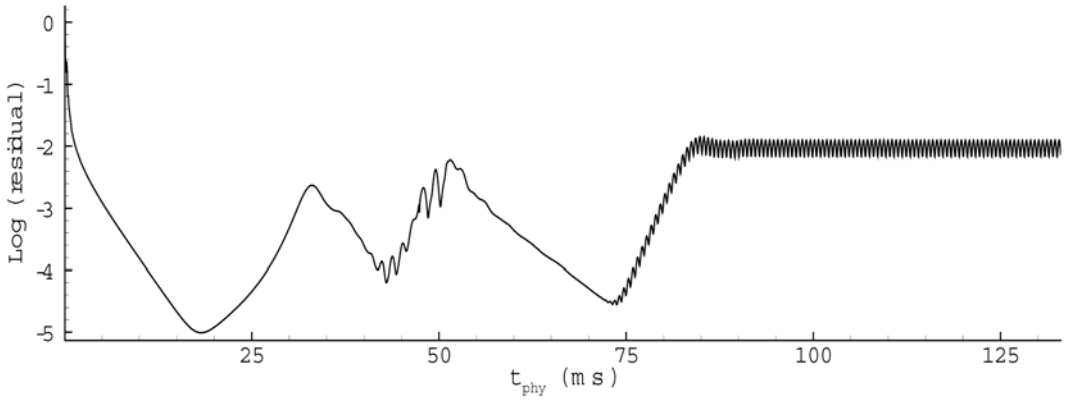

Figure 8: Residual time evolution, *Lz*=1

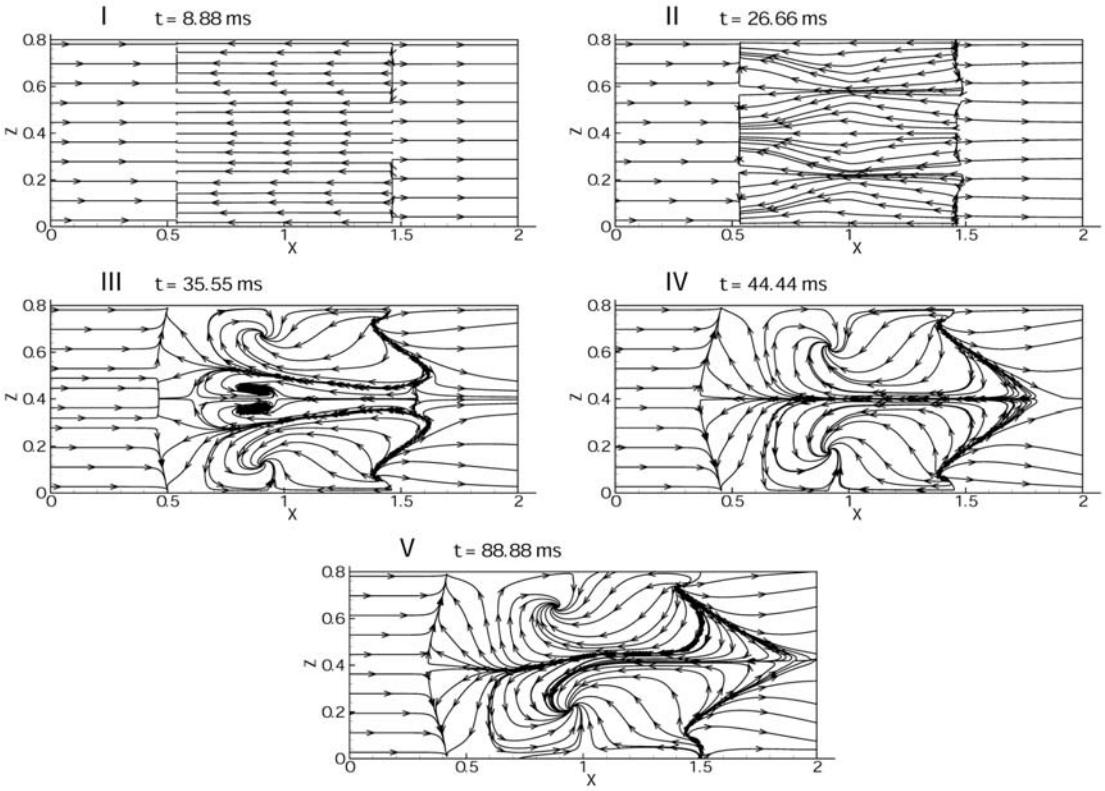

Figure 9: Surface streamlines on the plate at different moments, *Lz*=0.8

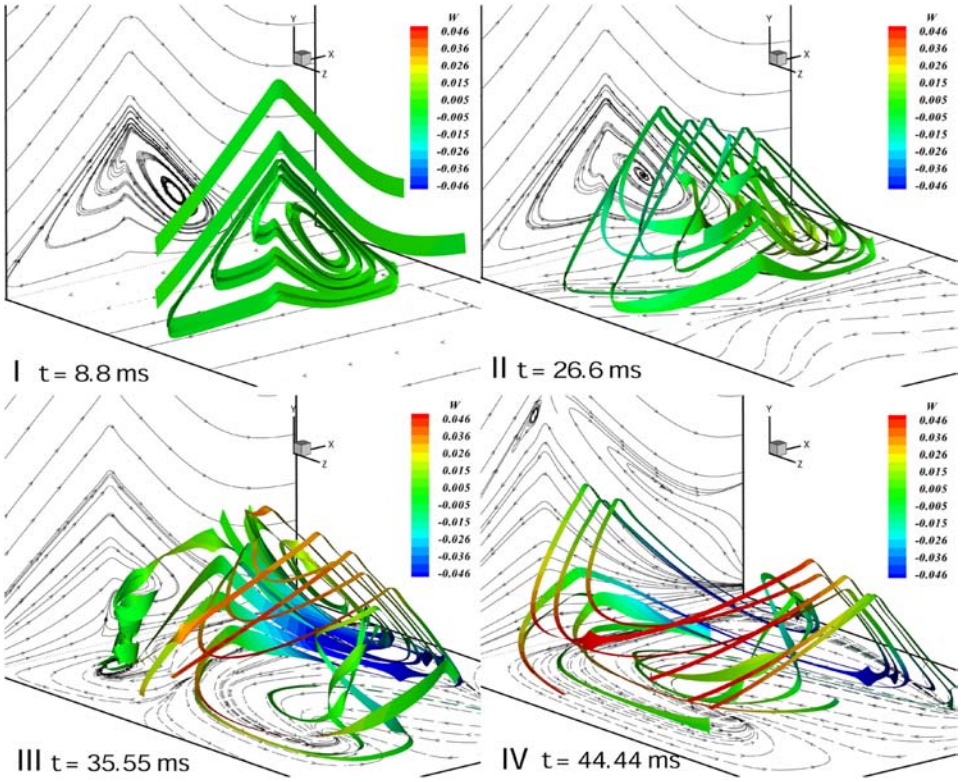

Figure 10: 3D views inside the bulb at different moments, *Lz*=0.8

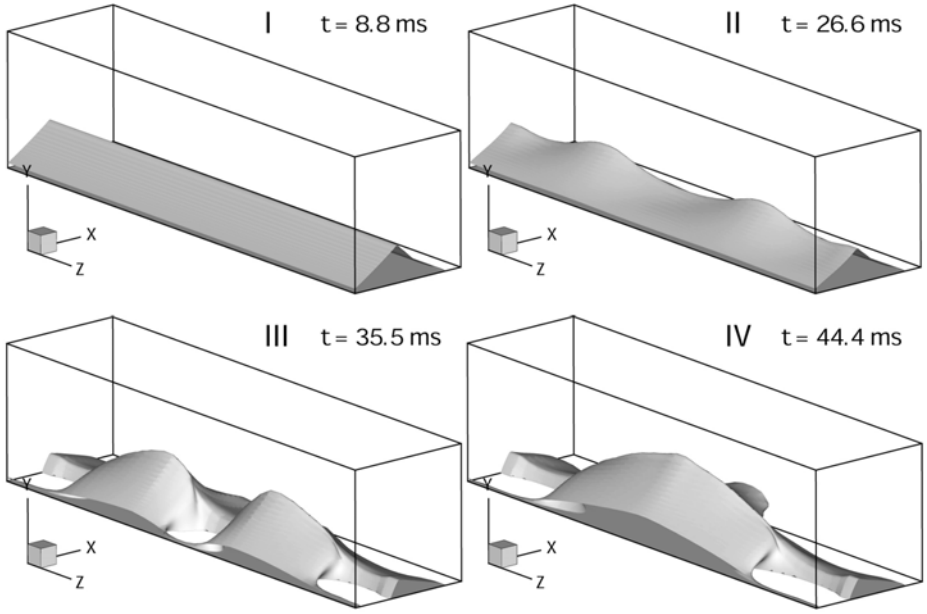

Figure 11: Bulb envelope at different moments, *Lz*=0.8

New computations have been performed for spanwise length equal to 2 and 3. We limit here to time corresponding to the first 3D steady bifurcation. We want to show that the instabilities transverse wavelengths are independent of the spanwise dimension *Lz*. Figure 12 shows surface streamlines for *Lz*=2. We note that the observed structures repeat three times instead of two times for *Lz*=0.8 or *Lz*=1. To confirm these observations, we compare the z-component of the friction coefficient Cf_z on the plate for *Lz*=2 and *Lz*=3, Figure 13. The dotted lines represent negative values of Cf_z , it alternates with positive values periodically. From theses figures, we can calculate the wavelength of the 3D instabilities: It is equal to 2/3 in the first case and 3/5 in the second. So the wavelength of the main 3D steady instability must be about 0.6 times the interaction length X_{sh}.

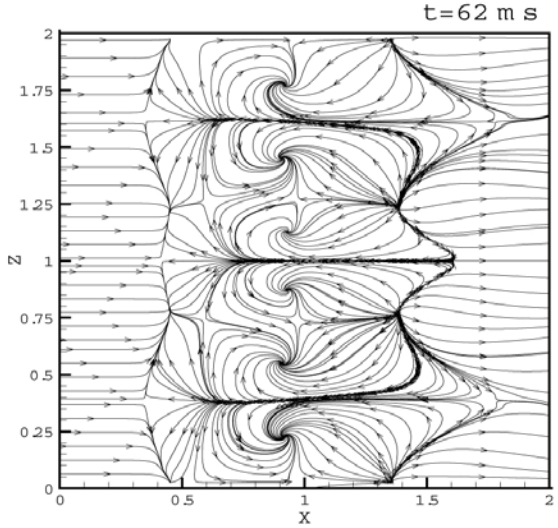

Figure 12: Surface streamlines on the plate at *t*=62ms, *Lz*= 2

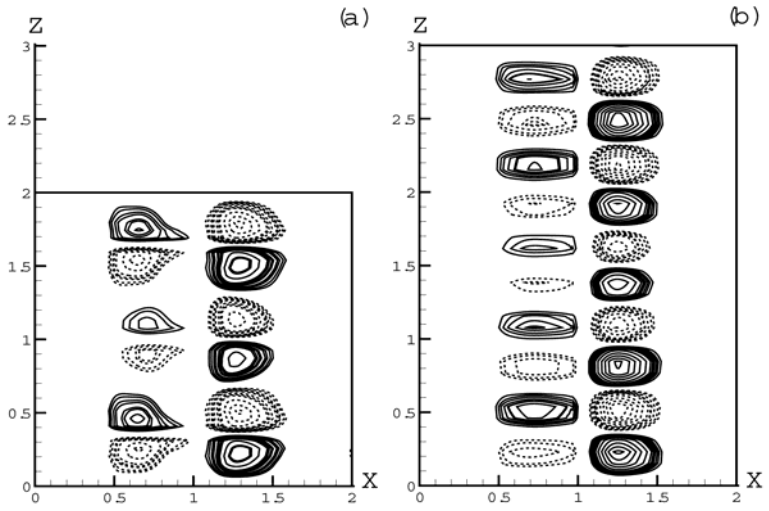

Figure 13: z-component of the friction coefficient on the plate, *Lz*=2 (a), *Lz*=3 (b)

4.0 CONCLUSIONS

This study has shown that self-sustained low frequency oscillations can appear in a strictly laminar SWBLI without upstream perturbations. These calculations highlighted a complex process in the installation of unsteady dynamics when the angle of the incident shock increases. Indeed, three-dimensional calculations have shown that before becoming unsteady, the SWBLI goes through a phase where the flow becomes three-dimensional and stationary (for θ>31°7). However, this state is unstable and can lead to a fully three-dimensional and unsteady flow. The final state is reached all the more quickly as the angle of the incident shock is large. When transverse dimension L_z is large enough, the flow has a principal transverse wavelength of $\lambda_z \approx 1$. In the interaction, the topology of the bulb is complex and transversely mainly characterized by cells where the flow is alternatively separated and reattached. Within the separated zones, the flow can take very complex forms but is mainly characterized by vortex waterspouts, the latter connecting the flow to the wall and the downstream shear layer from the interaction. This successive process of bifurcations from a stationary two-dimensional flow to an unsteady three-dimensional final state while passing by the intermediate stationary three-dimensional but unstable states can be interpreted like a driving scenario with the onset of the vortex shedding phenomenon. Indeed, U. Dallmann [7] observed in incompressible separated flows that the vortex shedding phenomenon was preceded by a three-dimensionalization of the flow associated with the break-up of saddle-connections. Figure 14 presents the Dallmann's conjecture. This conjecture proposes that before the flow is unsteady and that the vortex-shedding appear, the multiple recirculation zones occur inside the primary bubble which finally lead to a global structural flow change with multiple structurally unstable saddle-to-saddle connections. Theofilis *et al.* [6] have recently established a link, within the framework of an incompressible flow, between the existence of three-dimensional global instabilities and the Dallmann's conjecture. We think that this conjecture can extend to separated supersonic flows and in particular with a SWBLI. This generalized conjecture could make it possible to understand the first stage, at least, of the establishment of the unsteady low frequency character in a SWBLI.

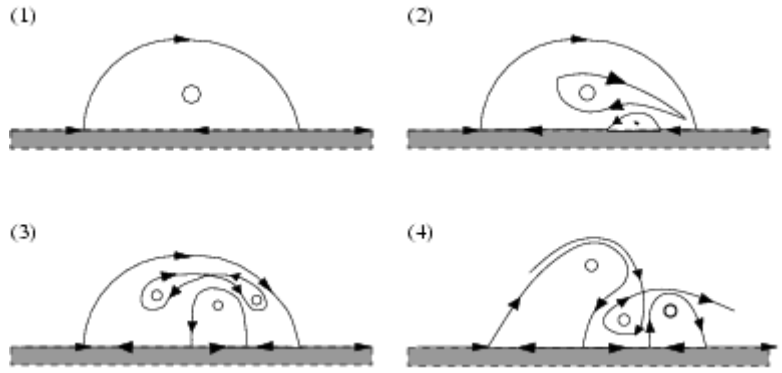

Figure 14: Conjecture for topological changes of a separation bubble's structure associated with the onset of vortex shedding.

REFERENCES

[1] J.-P. Boin, J.-Ch. Robinet, C. Corre, H. Deniau, 2004, "3D steady and unsteady bifurcations in a laminar shock-wave / boundary layer interaction; a numerical study", Physic of Fluids, submitted April 2004.

[2] Degrez G., Boccadoro C. H., Wendt J. F., 1987, "The interaction of an oblique shock wave with a laminar boundary layer revisited. An experimental and numerical study", J. Fluid Mech., Vol. 177, pp. 247-263

[3] Edwards J. and Liou M.S., 1998, "Low-diffusion flux-splitting methods for flows at all speeds", AIAA J. vol. 36, pp. 1610-1617

[4] Dolling D. S., 2001, "Fifty Years of Shock-Wave / Boundary-Layer Interaction Research: What Next ?, AIAA J., Vol. 39, N°8

[5] P. Dupont, J.F. Debiève, C. Haddad, J.P. Dussauge, 2004, "Three-dimensional organization and unsteadiness of a shock wave/turbulent boundary layer interaction", ISSW-04 - Sendai, Japan

[6] Theofilis V., Hein S., Dallmann U., 2000, "On the origins of unsteadiness and three-dimensionality in a laminar separation bubble", Phil. Trans. R. Soc. Lond. A., pp. 3229-3246

[7] Dallman U., 1988 "Three-dimensional vortex structures and vorticity topology", In Proc. IUTAM Symposium on "Fundamental aspects of vortex motion", Tokyo, Japan, 183-189